International Forum on Aeroelasticity and Structural Dynamics
IFASD 2024
17-21 June 2024, The Hague, The Netherlands

DYNAMIC ANALYSIS OF NONLINEAR AEROSERVOELASTICITY BY A MODIFIED FREQUENCY–TIME DOMAIN METHOD

Peihan Wang[1], **Zhigang Wu**[*1], **Chao Yang**[1,2]

[1] School of Aeronautic Science and Engineering, Beihang University
37 Xueyuan Road, Haidian District, Beijing 100191, China
wuzhigang@buaa.edu.cn

[2] International Innovation Institute, Beihang University
166 Shuanghongqiao Street, Pingyao Town, Yuhang District, Hangzhou 311115, China

Keywords: Aeroservoelasticity, Nonlinear dynamics, Frequency–time domain method

Abstract: Dynamic analysis of nonlinear aeroservoelastic systems has been a subject of concern for decades. A modified frequency–time domain method is competent in analyzing nonlinear aeroelastic systems, with the capability of addressing various nonlinearities and initial conditions. An extension of this method is presented to allow nonlinear responses of closed-loop systems with freeplay and actuator nonlinearities. Aeroservoelastic systems can be reconstructed by extracting nonlinear elements as pseudo forces in the nonlinear feedback loops in the time domain, whereas the original feedback loops are also introduced via the convolution integral. Hence, nonlinear responses with various nonlinearities and initial conditions can be obtained by the proposed method. Numerical results are provided for a three-degree-of-freedom airfoil section with freeplay and actuator nonlinearities, which is augmented to an aeroservoelastic system. Compared with the Runge–Kutta algorithm, the feasibility and accuracy of the proposed method can be validated. As an alternative to time-marching approaches, the modified frequency–time domain method initiates a novel process to address various nonlinearities and initial conditions in nonlinear aeroservoelastic systems.

1 INTRODUCTION

Dynamic analysis plays a pivotal role in aeroservoelasticity [1], exhibiting the intricate interactions between aerodynamics, structural dynamics, and control systems. However, nonlinearities [2] pose further challenges to analyze in aeroservoelastic (ASE) systems. Herein, nonlinearities, constituting aerodynamic, structural, and control ones, have significant impacts on the stability and dynamic responses.

One of the most ubiquitous nonlinearities, structural freeplay [3, 4], has been investigated from aeroelastic to ASE systems for decades. Tang and Dowell [5] explored the effect of control surface freeplay in a typical aeroelastic airfoil section, thereby allowing nonlinear responses with gust excitation. Furthermore, a three-degree-of-freedom (DOF) aeroelastic system with freeplay was analyzed by Candon et al. [6, 7], with higher-order spectra techniques and the Hilbert-Huang transform to unveil features of systems with both aerodynamic and structural nonlinearities. Wang et al. [8] proposed a dual quasi-harmonic balance method to investigate three-domain limit cycles in a three-dimensional wing-aileron model with freeplay. For nonlinear ASE systems, Gold and Karpel [9] reconstructed nonlinear models via the fictitious mass approach to observe nonlinear responses with freeplay, regarded as structural nonlinearities of

actuators, to conduct stability analysis and maneuver simulations. Furthermore, this modeling method was extended to a three-dimensional multiple-actuated-wing case by Huang et al. [10] to indicate the effect of freeplay in nonlinear ASE systems. Based on component mode synthesis techniques, Tian et al. [11] analyzed a three-dimensional supersonic aircraft with freeplay and presented a hybrid adaptive feedback control algorithm for gust load alleviation.

Numerous methods have been developed to analyze nonlinear systems in different calculation domains, i.e., the frequency and time domains. The frequency-domain approaches, as semi-analytical methods, are proficient at addressing various nonlinearities; however, the accuracy of classical ones is unsatisfactory [12]. Contrastingly, the time-marching approaches, namely numerical methods, are competent in complex nonlinear systems. However, these methods are tedious and computationally intensive [3], notably when the time step is a significant factor in the accuracy of nonlinear responses. Owing to the preceding drawbacks, the frequency–time domain methods were proposed, for instance, the hybrid frequency–time domain approach [13] and alternating frequency/time domain method [14]. Herein, these methods address nonlinearities in the time domain and merge features in both the frequency and time domain. Based on these characteristics, Karpel et al. [15, 16] proposed the increased-order modeling (IOM) approach to circumvent rational function approximation techniques that compromise accuracy. Thereafter, Karpel and his colleagues extended the IOM approach to various applications [17, 18], indicating its merits. Furthermore, Owing to the significant impact of initial conditions, Wang et al. [19] modified the IOM approach to exhibit nonlinear transient responses in two-dimensional aeroelastic systems. The modification extended the IOM approach to allow transient nonlinear responses and highlighted the capability of handling various nonlinearities. However, many challenges remain for the application of this modified method in ASE systems.

Based on the aforementioned research, an attempt is made to extend the modified frequency–time domain method to investigate nonlinearities in ASE systems. The aeroelastic parts of closed-loop systems can be separated into the main linear block and nonlinear feedback loops; furthermore, actuators are also partitioned in a commensurate manner. Additionally, the original feedback loops can be reconstructed, similar to the nonlinear feedback loops. Owing to the capability of addressing various nonlinearities and initial conditions, the modified frequency–time domain method can be applied to explore nonlinear systems with both freeplay and actuator nonlinearities. Therefore, nonlinear responses can be obtained by the proposed method. A three-DOF airfoil typical section with control surface freeplay and actuator nonlinearities is utilized to validate the feasibility and accuracy of the proposed method, compared with the Runge–Kutta algorithm.

2 THE MODIFIED FREQUENCY–TIME DOMAIN METHOD

A modified frequency–time domain method [19] was presented to deal with various nonlinearities and initial conditions in nonlinear systems, based on the IOM approach [17, 18].

The equation of nonlinear systems can be expressed as

$$\mathbf{M}\ddot{\mathbf{x}}(t) + \mathbf{C}\dot{\mathbf{x}}(t) + \mathbf{K}\mathbf{x}(t) = \mathbf{f}(t) + \mathbf{u}(t) \tag{1}$$

where $\mathbf{x}$, $\dot{\mathbf{x}}$ and $\ddot{\mathbf{x}}$ are nonlinear responses and their time derivatives. $\mathbf{M}$, $\mathbf{C}$ and $\mathbf{K}$ are mass, damping, and stiffness coefficient matrices, respectively. $\mathbf{f}(t)$ are external forces and $\mathbf{u}(t)$ are pseudo forces representing nonlinear elements.

Considering initial conditions, the equation is rearranged as

$$\mathbf{M}\ddot{\bar{\mathbf{x}}}(t) + \mathbf{C}\dot{\bar{\mathbf{x}}}(t) + \mathbf{K}\bar{\mathbf{x}}(t) = \mathbf{f}(t) + \tilde{\mathbf{u}}(t) \tag{2}$$

where $\tilde{\mathbf{u}}(t)$ are the extension of pseudo forces constituting nonlinear elements and initial conditions, expressed as

$$\tilde{\mathbf{u}}(t) = \mathbf{u}(t) - \mathbf{K}(\mathbf{x_0} + \dot{\mathbf{x}}_\mathbf{0} t) - \mathbf{C}\dot{\mathbf{x}}_\mathbf{0} \tag{3}$$

where $\mathbf{x_0}$, $\dot{\mathbf{x}}_\mathbf{0}$ are initial displacements and velocities.

Based on the frequency–time domain method, nonlinear systems are divided into main linear blocks and nonlinear elements, shown in Figure 1.

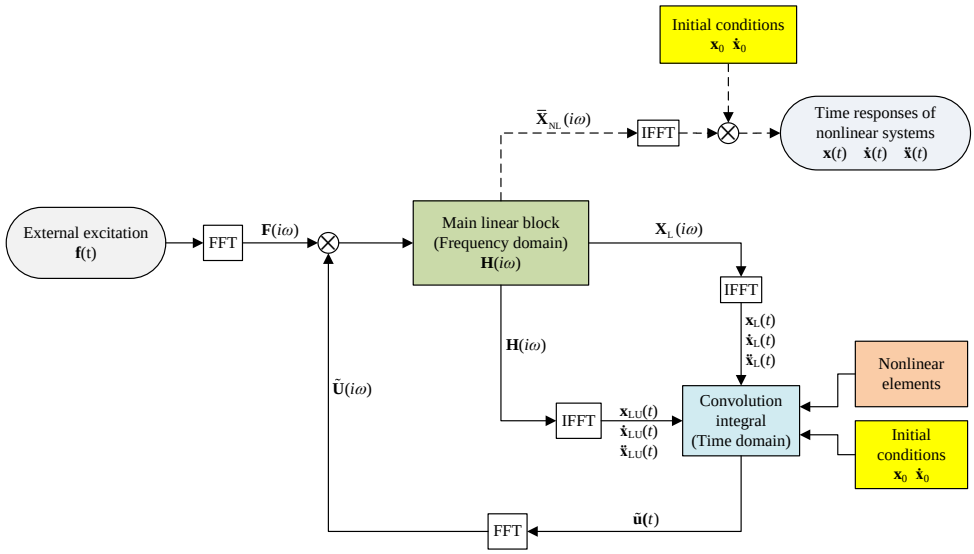

Figure 1: The detailed flow chart of the modified IOM method [19].

Herein, the main linear blocks are calculated in the frequency domain, eliminating $\tilde{\mathbf{u}}(t)$ in Eq.2. The equations can be presented as

$$\begin{aligned} \bar{\mathbf{x}}_\mathrm{L}(\mathrm{i}\omega) =& [-\omega^2\mathbf{M} + \mathrm{i}\omega\mathbf{C} + \mathbf{K}]^{-1}\mathbf{F}(\mathrm{i}\omega) \\ \mathbf{H}(\mathrm{i}\omega) =& [-\omega^2\mathbf{M} + \mathrm{i}\omega\mathbf{C} + \mathbf{K}]^{-1} \end{aligned} \tag{4}$$

where $\bar{\mathbf{x}}_\mathrm{L}(\mathrm{i}\omega)$ and $\mathbf{H}(\mathrm{i}\omega)$ are frequency responses induced by external forces and impulse, respectively. $\mathbf{F}(\mathrm{i}\omega) = \mathscr{F}(\mathbf{f}(t))$ are the frequency-domain counterparts of external forces. $\mathscr{F}$ and $\mathscr{F}^{-1}$ are the respective symbols of fast Fourier transform (FFT) and inverse fast Fourier transform (IFFT).

Thereafter, the frequency responses can be transformed into the time domain, expressed as

$$\begin{aligned} \bar{\mathbf{x}}_\mathrm{L}(t) =& \mathscr{F}^{-1}(\bar{\mathbf{x}}_\mathrm{L}(\mathrm{i}\omega)) \\ \bar{\mathbf{x}}_\mathrm{LU}(t) =& \mathscr{F}^{-1}(\mathbf{H}(\mathrm{i}\omega)) \end{aligned} \tag{5}$$

where $\bar{\mathbf{x}}_\mathrm{L}(t)$ and $\bar{\mathbf{x}}_\mathrm{LU}(t)$ are the corresponding linear responses.

Based on the aforementioned linear responses, the convolution integral, shown in Figure 2, is represented as

$$\mathbf{x}(t) = \mathbf{x}_\mathrm{L}(t) + \int_0^{t_\mathrm{NL}} \mathbf{x}_\mathrm{LU}(t-\tau)\tilde{\mathbf{u}}(\tau)d\tau \tag{6}$$

where $\tilde{\mathbf{u}}$ can also be nonlinear functions of responses, which are constructed by pseudo forces of nonlinear elements and initial conditions in Eq.(3), expressed as

$$\tilde{\mathbf{u}} = F_{\mathrm{NL}}(\mathbf{x}, \dot{\mathbf{x}}, \ddot{\mathbf{x}}) \tag{7}$$

where F_{NL} is the expression of the nonlinear functions.

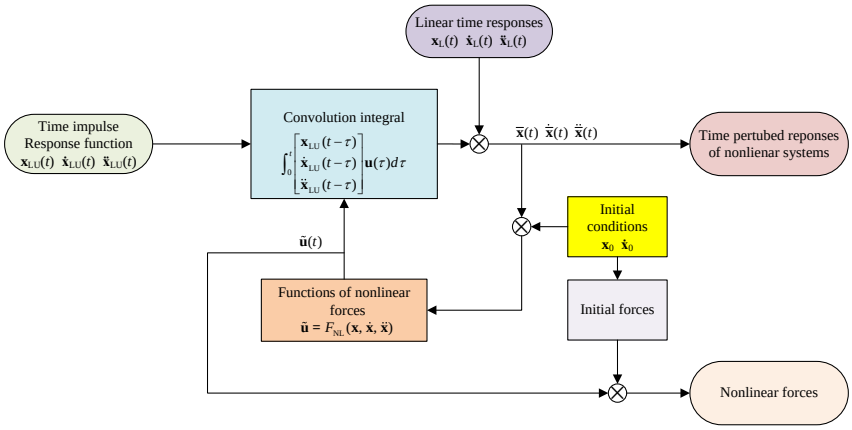

Figure 2: The modified expression of convolution integral [19].

Herein, $\tilde{\mathbf{u}}$ can be transformed into the frequency domain, as $\tilde{\mathbf{U}}(\mathrm{i}\omega) = \mathscr{F}(\tilde{\mathbf{u}}(t))$, to compute the frequency-domain counterparts of nonlinear time responses.

3 THE MODIFICATION FOR NONLINEAR AEROSERVOELASTIC SYSTEMS

Owing to the capability of addressing various nonlinearities and initial conditions, the modified frequency–time domain method can be extended to the application for nonlinear ASE systems, as shown in Figure 3. For instance, two types of nonlinearities, freeplay and actuator nonlinearities, are presented, which are ubiquitous in ASE systems.

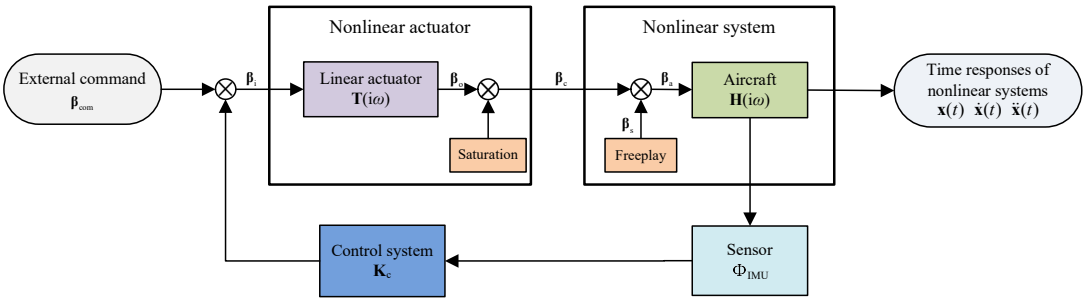

Figure 3: Sketch of nonlinear Aeroservoelastic systems.

The equation in Eq.(1) reflects the characteristics of nonlinear aeroelastic systems; moreover, the deflection of control surfaces $\boldsymbol{\beta}$ is part of the state variables $\mathbf{q}$ thereof. Furthermore, actuators and control systems are augmented, thereby extending aeroelastic systems to ASE ones.

For simplicity, control systems are represented as gain $\mathbf{K}_c$ to examine nonlinearities. Herein, freeplay is introduced in aeroelastic systems per se, whereas actuator nonlinearities are considered in the process of construction, regarded as the saturation of deflection and rate. Therefore, nonlinear actuators in the ASE systems are represented as

$$\boldsymbol{\beta}_c(t) = T_{\mathrm{NL}}(\boldsymbol{\beta}_i) \tag{8}$$

where $\boldsymbol{\beta}_{\mathrm{i}}$, $\boldsymbol{\beta}_{\mathrm{c}}$ are the respective inputs and outputs of nonlinear actuators. T_{NL} is the expression of the corresponding nonlinear functions.

Notably, nonlinear actuators can be partitioned into linear and nonlinear parts, resembling the aeroelastic systems. The nonlinear parts can be introduced in the time domain, whereas the linear ones can be presented as the transfer functions $\mathbf{T}(s)$ in the frequency domain, given as

$$\boldsymbol{\beta}_{\mathrm{o}} = \mathbf{T}(s)\boldsymbol{\beta}_{\mathrm{i}} \tag{9}$$

where $\boldsymbol{\beta}_{\mathrm{o}}$ are the outputs of linear parts.

Owing to the characteristics of the frequency–time domain method, the impacts of two distinct nonlinearities can be observed from nonlinear responses in conjunction. However, the modification should be conducted to introduce two types of nonlinearities in nonlinear ASE systems. The details of applying the proposed method are represented in this section.

3.1 Freeplay

Owing to closed-loop systems, the inputs to original aeroelastic systems are the actual angles of control surfaces $\boldsymbol{\beta}_{\mathrm{a}}$, constituting the deflections of springs hinged with the control surfaces $\boldsymbol{\beta}_{\mathrm{s}}$ and the outputs of actuators $\boldsymbol{\beta}_{\mathrm{c}}$, expressed as

$$\boldsymbol{\beta}_{\mathrm{a}} = \boldsymbol{\beta}_{\mathrm{s}} + \boldsymbol{\beta}_{\mathrm{c}} \tag{10}$$

Freeplay exists when hinge moments of control surfaces change sign [9, 10], differing from the aeroelastic systems. Thereafter, responses of $\boldsymbol{\beta}_{\mathrm{s}}$ reflect freeplay of springs, shown in Figure 4, thereby obtaining nonlinear responses.

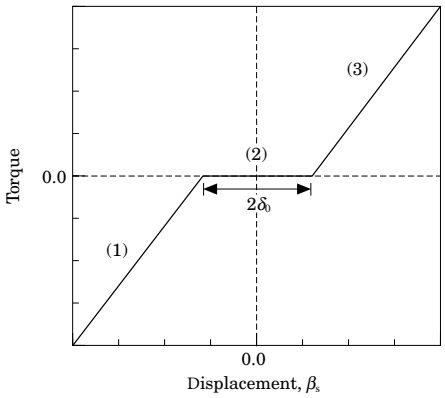

Figure 4: Freeplay nonlinearity [20].

Hence, when one of control surfaces β_{s} is induced by freeplay, the corresponding hinge moment M_β can be expressed as

$$M_\beta = \begin{cases} K_\delta(\beta_{\mathrm{s}} + \delta_0) & \beta_{\mathrm{s}} < -\delta_0 \\ 0 & -\delta_0 \leq \beta_{\mathrm{s}} \leq \delta_0 \\ K_\delta(\beta_{\mathrm{s}} - \delta_0) & \beta_{\mathrm{s}} > \delta_0 \end{cases} \tag{11}$$

where δ_0 is the angular size of freeplay.

3.2 Actuator nonlinearities

Based on actual mechanical systems of actuators, the deflection and rate of control surfaces driven by actuators are restricted, presented as

$$\begin{cases} |\boldsymbol{\beta}_{\mathrm{o}}| \leq \mathbf{x}_{\mathrm{lim}} \\ |\dot{\boldsymbol{\beta}}_{\mathrm{o}}| \leq \mathbf{v}_{\mathrm{lim}} \end{cases} \tag{12}$$

where $\mathbf{x}_{\mathrm{lim}}$ and $\mathbf{v}_{\mathrm{lim}}$ are the maximum deflection and rate of control surfaces corresponding to nonlinear actuators, respectively.

Owing to the complexity of nonlinear actuators, the linear outputs $\boldsymbol{\beta}_{\mathrm{o}}$ can be rearranged into the actual outputs $\boldsymbol{\beta}_{\mathrm{c}}$ by the saturation of deflection and rate. Furthermore, the actual deflections $\boldsymbol{\beta}_{\mathrm{a}}$ can be computed, combining $\boldsymbol{\beta}_{\mathrm{c}}$ with $\boldsymbol{\beta}_{\mathrm{s}}$.

3.3 The modification of the frequency–time domain method

Owing to the capability of addressing various nonlinearities, the frequency–time domain method can be extended to the application for nonlinear ASE systems. The introduction of isolated linear components [16] in the convolution integral is applied to reconstruct the original feedback loops.

Based on Section 2, nonlinear actuators are partitioned into linear and nonlinear parts, the linear of which in Eq.(9) are transformed into the time domain by IFFT, given as

$$\begin{aligned} \bar{\mathbf{t}} &= \mathscr{F}^{-1}(\mathbf{T}(\mathrm{i}\omega)) \\ \dot{\bar{\mathbf{t}}} &= \mathscr{F}^{-1}(\mathrm{i}\omega\mathbf{T}(\mathrm{i}\omega)) \end{aligned} \tag{13}$$

where $\bar{\mathbf{t}}$, $\dot{\bar{\mathbf{t}}}$ are time impulse response functions and their derivatives of actuators.

Owing to the augmentation of actuators and control systems, the extra convolution integral of $\boldsymbol{\beta}_{\mathrm{o}}$ should be computed, represented as

$$\boldsymbol{\beta}_{\mathrm{o}} = \int_0^{t_{\mathrm{NL}}} \bar{\mathbf{t}}(t-\tau)\boldsymbol{\beta}_{\mathrm{i}}(\tau)d\tau \tag{14}$$

where t_{NL} is the ending time for convolution integral.

For nonlinear ASE systems, the functions of nonlinear forces are rearranged as

$$\tilde{\mathbf{u}} = F_{\mathrm{NL}}(\mathbf{x}, \dot{\mathbf{x}}, \ddot{\mathbf{x}}, \boldsymbol{\beta}_{\mathrm{o}}) \tag{15}$$

In the aforementioned section, the reconstruction of nonlinear ASE systems is conducted to introduce various nonlinearities in the time domain, thereby computing nonlinear responses.

4 NUMERICAL RESULTS

Based on the modification for nonlinear ASE systems, a three-DOF aeroelastic typical section with control surface freeplay [20] is presented, shown in Figure 5, to validate the feasibility and accuracy.

The dynamic equation of the aeroelastic case is represented as

$$\bar{\mathbf{M}}\ddot{\mathbf{x}} + \bar{\mathbf{C}}\dot{\mathbf{x}} + \bar{\mathbf{K}}\mathbf{x} = \bar{\mathbf{G}} \tag{16}$$

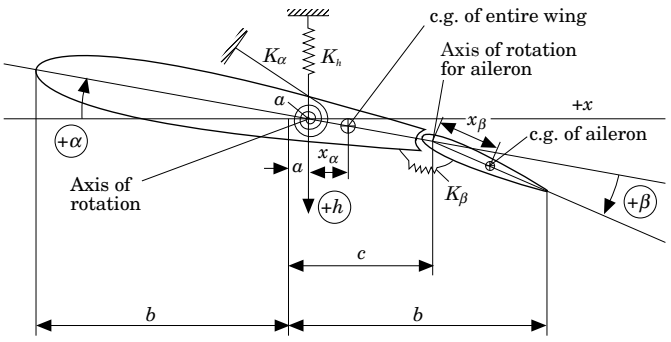

Figure 5: Three-DOF aeroelastic typical section [20].

where $\mathbf{x} = [\alpha \quad \beta_\mathrm{a} \quad h/b \quad x_\mathrm{a}]^\mathrm{T}$ are state-space variables. Herein, α and β_a are the respective angles of pitch and flap deflection. h is the plunge displacement, and x_a is the augmented state. b is the semi-chord of wing. $\bar{\mathbf{G}}$ are the pseudo forces induced by freeplay. $\bar{\mathbf{M}}$, $\bar{\mathbf{C}}$ and $\bar{\mathbf{K}}$ are the respective mass, damping and stiffness coefficient matrices, given as

$$\begin{aligned}
\bar{\mathbf{M}} &= \begin{bmatrix} \mathbf{M} & \mathbf{0} \\ \mathbf{0} & 1 \end{bmatrix} \\
\bar{\mathbf{C}} &= \begin{bmatrix} \mathbf{C} & -(c_1c_2 + c_3c_4)\frac{\rho U^2}{m}\mathbf{R} \\ -\mathbf{S}_2 & (c_2 + c_4)\frac{U}{b} \end{bmatrix} \\
\bar{\mathbf{K}} &= \begin{bmatrix} \mathbf{K} & -c_2c_4(c_1 + c_3)\frac{\rho U^3}{mb}\mathbf{R} \\ -\frac{U}{b}\mathbf{S}_1 & c_2c_4\frac{U^2}{b^2} \end{bmatrix}
\end{aligned} \tag{17}$$

where m is the mass of wing and flap, and ρ is the sir density. U is the freestream velocity, and $c_1 = 0.165$, $c_2 = 0.0455$, $c_3 = 0.335$, $c_4 = 0.3$ are the constants related to unsteady aerodynamics [21, 22]. $\mathbf{M}$, $\mathbf{C}$, $\mathbf{K}$ are the matrices involving structural and aerodynamic components. The details of these matrices and parameters are presented as Case C in [19].

Augmented with an actuator and a control system, a nonlinear ASE system can be constructed in Figure 6. The actual flap deflection β_a consists of the output of the actuator β_c and the rotation of the spring-hinged with the flap β_s, which resembles Eq.(10). To validate the proposed method, both linear and nonlinear parts of actuators are introduced in this two-dimensional case. The linear part can be presented in the frequency domain, whose transfer function is expressed as

$$T(s) = \frac{1}{as + 1} = \frac{\beta_\mathrm{o}}{\beta_\mathrm{i}} \tag{18}$$

where $a = 0.0318$ is the constant. Owing to the single control surface in this case, the corresponding variables are simplified from vectors to scalars.

Furthermore, actuator nonlinearities, the saturation of deflection and rate, are introduced in the time domain by restricting the linear output β_o in Eq.(14) to the output β_c suitable for actual nonlinear actuators. The limitations of maximum deflection and rate can be represented as Eq.(12).

Thereafter, the feedback of pitch rate $\dot{\alpha}$ is adopted as the control system to construct the closed-loop system, whose gain is represented as $K_\mathrm{c} = 0.05$. Hence, the input to the linear part of the actuator is expressed as

$$\beta_\mathrm{i} = K_\mathrm{c}\dot{\alpha} + \beta_\mathrm{com} \tag{19}$$

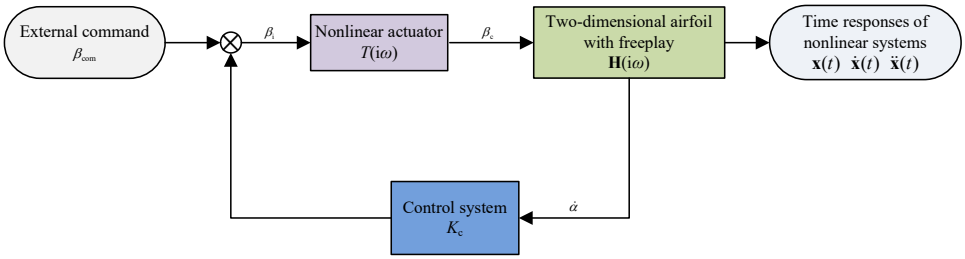

Figure 6: The three-DOF nonlinear ASE system.

where β_{com} is the input of a command to the actuator.

Herein, freeplay and actuator nonlinearities are individually introduced into the ASE system, thereby allowing nonlinear responses by the modified frequency–time domain method. Furthermore, responses induced by two types of nonlinearities can be obtained. The given conditions are freestream velocity $U = 10.08$ m s^{-1} and air density ρ = 1.225 kg m^{-3}.

4.1 Freeplay

The nonlinear ASE system is constructed to simulate nonlinear responses induced by freeplay δ_0 = 1.15 deg, eliminating actuator nonlinearities. Responses with initial conditions of h/b = 0.04 and zero are computed by the proposed method, shown in Figure 7. It is recognized that the results of the proposed method are in good agreement with those of the Runge-Kutta algorithm, which validates the feasibility and accuracy of the former. Results of various sampling frequencies indicate that the modification for ASE systems intensifies the sensitivity to sampling frequency, the lower of which leads to less accuracy.

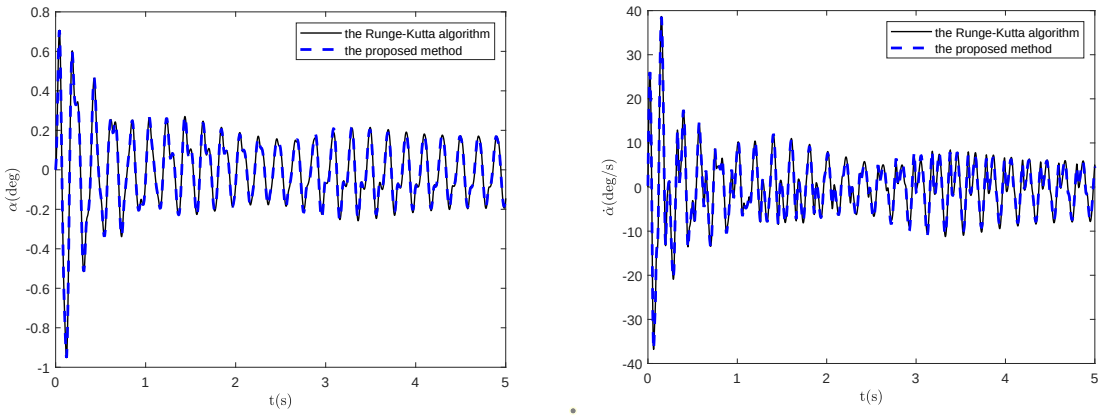

(a) pitch angle (b) pitch rate

Figure 7: Responses with freeplay and initial conditions h/b = 0.04

4.2 Actuator nonlinearities

Closed-loop systems exhibit nonlinear responses due to the additional nonlinearities induced by actuators and control systems. The most ubiquitous components are the saturation of deflection and rate, which are introduced into the nonlinear feedback loops to validate the feasibility and accuracy of the proposed method. Two Signals are designated as the commands in Figure 8, indicating the saturation of deflection x_{lim} = 60 deg and that of rate v_{lim} = 50 deg/s. Responses with saturation of actuator deflection are shown in Figure 9, induced by the command in Figure

8 (a). The proposed method produces consistent results with the Runge-Kutta algorithm, which demonstrates the feasibility and accuracy of the former. Furthermore, the signal of command in Figure 8 (b) is induced to explore the rate saturation. Correspondingly, responses in Figure 10 reveal the feasibility and accuracy of the proposed method.

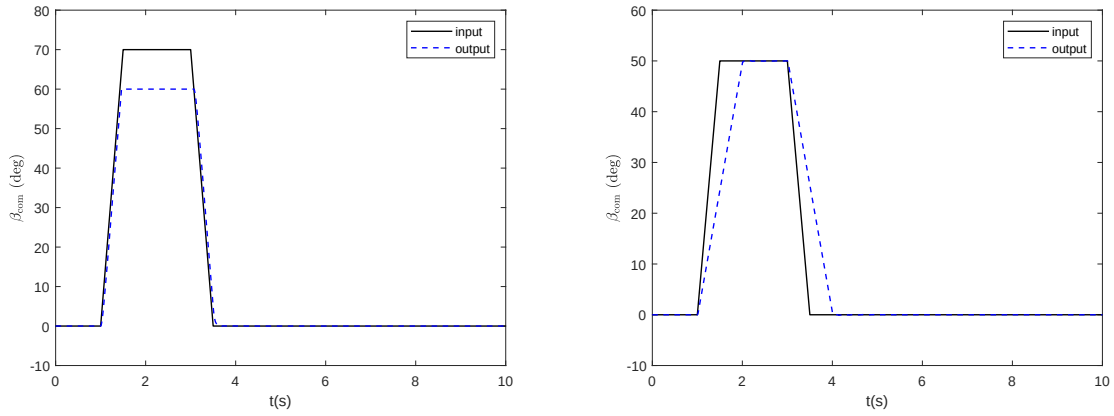

(a) Command for saturation of deflection (b) Command for saturation of rate

Figure 8: Signals of command for deflection limitation.

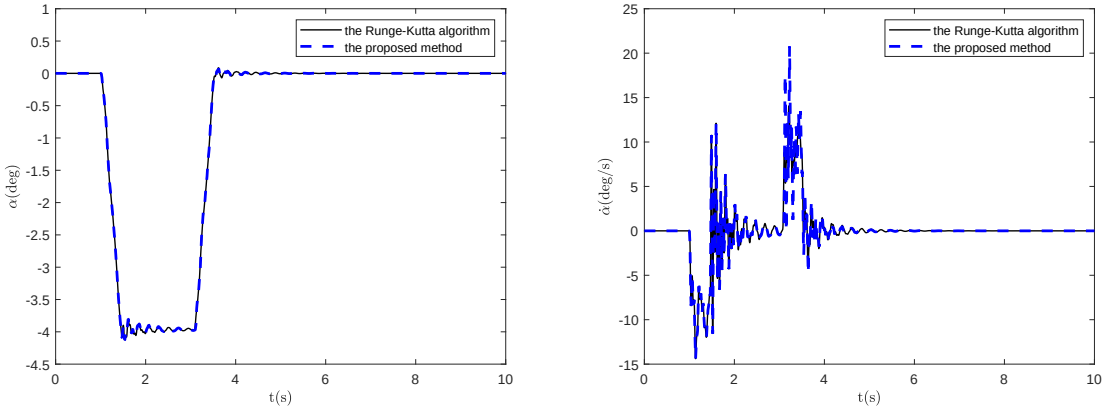

(a) pitch angle (b) pitch rate

Figure 9: Responses with command and saturation of deflection

4.3 Two types of nonlinearities

In the aforementioned simulations, the effects of both freeplay and actuator nonlinearities can individually be introduced by the modified frequency–time domain method. Herein, two types of nonlinearities are jointly presented in the ASE system.

Nonlinear responses with initial conditions h/b = 0.1 in Figure11 demonstrate the feasibility and accuracy of the proposed method, compared with the Runge–Kutta algorithm. However, the slight discrepancy is exhibited, as time progresses. Furthermore, the results induced by command indicate the feasibility and accuracy of the proposed method, without discrepancy of responses with initial conditions.

The preceding observation reveal that the modified frequency–time domain method is proficient at addressing both freeplay and actuator nonlinearities in conjunction, thereby obtaining

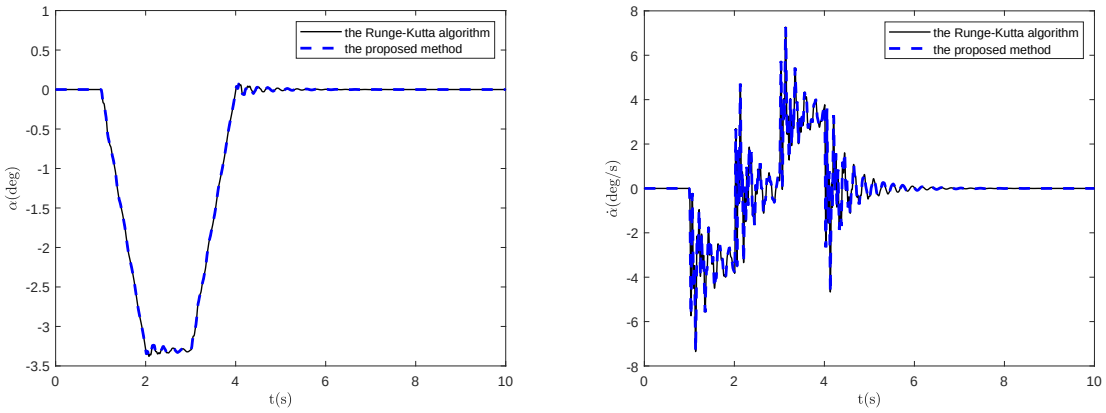

(a) pitch angle (b) pitch rate

Figure 10: Responses with command and saturation of rate

nonlinear responses induced by either command or initial conditions.

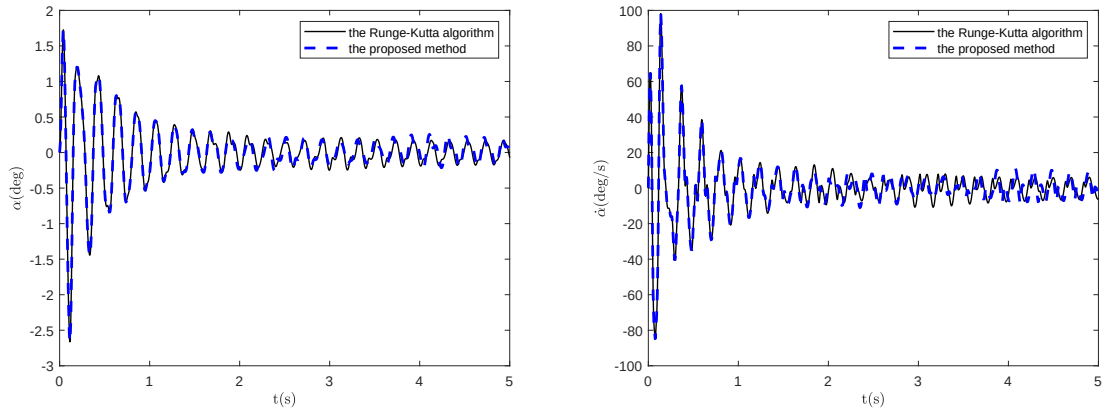

(a) pitch angle (b) pitch rate

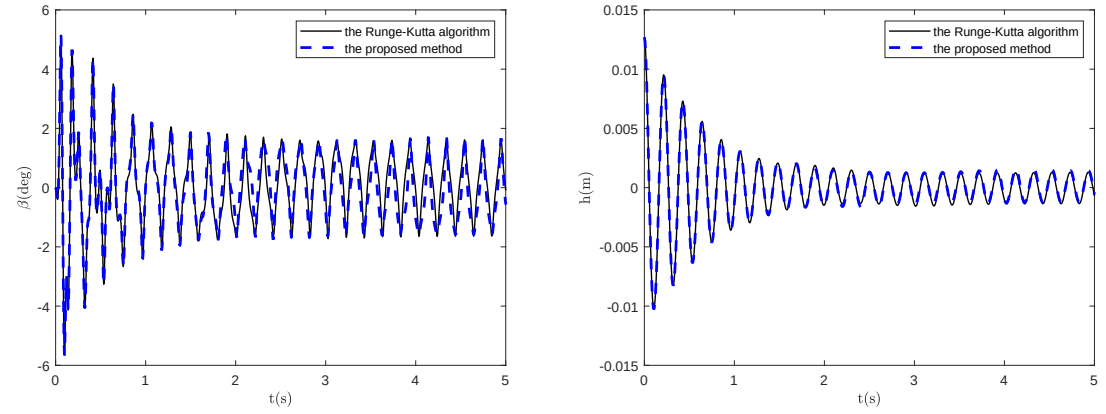

(c) flap displacement (d) plunge displacement

Figure 11: Responses with double nonlinearities and initial conditions $h/b = 0.1$

5 CONCLUSION

In this study, the modified frequency–time domain method is extended for nonlinear ASE systems to address various nonlinearities and initial conditions. Nonlinear ASE systems are re-

constructed by extracting nonlinear elements as pseudo forces to nonlinear feedback loops, whereas the original ones are also introduced in the time domain. Thereafter, the effects of both freeplay and actuator nonlinearities are embedded in nonlinear ASE systems, allowing nonlinear responses. Numerical results of a three-DOF typical airfoil section are conducted to explore the modified frequency–time domain method. Herein, different nonlinearities are individually or jointly introduced in closed-loop systems. The comparison with Runge–Kutta algorithm demonstrate the feasibility and accuracy of the proposed method, as an alternative to time-marching approaches. The modified frequency–time domain method proposes a novel formulation to address various nonlinearities and initial conditions, providing insights for stability analysis and dynamic response simulations of complex nonlinear systems.

6 REFERENCES

[1] Livne, E. (2018). Aircraft active flutter suppression: State of the art and technology maturation needs. *Journal of Aircraft*, 55(1), 410–452. doi:10.2514/1.C034442.

[2] Dowell, E. (2010). Some recent advances in nonlinear aeroelasticity: Fluid-structure interaction in the 21st century. In *51st AIAA/ASME/ASCE/AHS/ASC Structures, Structural Dynamics, and Materials Conference*. doi:10.2514/6.2010-3137.

[3] Panchal, J. and Benaroya, H. (2021). Review of control surface freeplay. *Progress in Aerospace Sciences*, 127, 100729. ISSN 0376-0421. doi:https://doi.org/10.1016/j.paerosci.2021.100729.

[4] Bueno, D. D., Wayhs-Lopes, L. D., and Dowell, E. H. (2022). Control-surface structural nonlinearities in aeroelasticity: A state of the art review. *AIAA Journal*, 60(6), 3364–3376. doi:10.2514/1.J060714.

[5] Tang, D. and Dowell, E. H. (2010). Aeroelastic airfoil with free play at angle of attack with gust excitation. *AIAA Journal*, 48(2), 427–442. doi:10.2514/1.44538.

[6] Candon, M., Carrese, R., Ogawa, H., et al. (2019). Characterization of a 3dof aeroelastic system with freeplay and aerodynamic nonlinearities – part i: Higher-order spectra. *Mechanical Systems and Signal Processing*, 118, 781–807. ISSN 0888-3270. doi:https://doi.org/10.1016/j.ymssp.2018.05.053.

[7] Candon, M., Carrese, R., Ogawa, H., et al. (2019). Characterization of a 3dof aeroelastic system with freeplay and aerodynamic nonlinearities – part ii: Hilbert–huang transform. *Mechanical Systems and Signal Processing*, 114, 628–643. ISSN 0888-3270. doi:https://doi.org/10.1016/j.ymssp.2018.04.039.

[8] Wang, X., Wu, Z., Sun, Y., et al. (2021). A novel method for estimating three-domain limit cycles in a 3d wing-aileron model with freeplay in aileron deflection. *Journal of Fluids and Structures*, 105, 103286. ISSN 0889-9746. doi:https://doi.org/10.1016/j.jfluidstructs.2021.103286.

[9] Gold, P. and Karpel, M. (2008). Reduced-size aeroservoelastic modeling and limit-cycle-oscillation simulations with structurally nonlinear actuators. *Journal of Aircraft*, 45(2), 471–477. doi:10.2514/1.28933.

[10] Huang, R., Hu, H., and Zhao, Y. (2013). Nonlinear aeroservoelastic analysis of a controlled multiple-actuated-wing model with free-play. *Journal of Fluids and Structures*, 42, 245–269. ISSN 0889-9746. doi:https://doi.org/10.1016/j.jfluidstructs.2013.06.007.

[11] Tian, W., Gu, Y., Liu, H., et al. (2021). Nonlinear aeroservoelastic analysis of a supersonic aircraft with control fin free-play by component mode synthesis technique. *Journal of Sound and Vibration*, 493, 115835. ISSN 0022-460X. doi:https://doi.org/10.1016/j.jsv.2020.115835.

[12] Ni, Y.-G., Zhang, W., and Lv, Y. (2020). A modified incremental harmonic balance method for 2-dof airfoil aeroelastic systems with nonsmooth structural nonlinearities. *Mathematical Problems in Engineering*, 2020, 5767451. ISSN 1024-123X. doi:10.1155/2020/5767451.

[13] Kawamoto, J. D. (1983). *Solution of nonlinear dynamic structural systems by a hybrid frequency-time domain approach*. Ph.D. thesis, Massachusetts Institute of Technology.

[14] Cameron, T. M. and Griffin, J. H. (1989). An alternating frequency/time domain method for calculating the steady-state response of nonlinear dynamic systems. *Journal of Applied Mechanics*, 56(1), 149–154.

[15] Karpel, M., Hollander, Y., Gur, I., et al. (2008). Increased-order models for the prediction of aeroelastic limit cycle oscillations. In *49th AIAA/ASME/ASCE/AHS/ASC Structures, Structural Dynamics, and Materials Conference, 16th AIAA/ASME/AHS Adaptive Structures Conference, 10th AIAA Non-Deterministic Approaches Conference, 9th AIAA Gossamer Spacecraft Forum, 4th AIAA Multidisciplinary Design Optimization Specialists Conference*. p. 1757.

[16] Karpel, M., Shousterman, A., Maderuelo, C., et al. (2009). Dynamic gust response with nonlinear control using frequency domain models. In *Proceedings of the International Forum on Aeroelasticity and Structural Dynamics*. pp. 2009–107.

[17] Reyes, M., Climent, H., Karpel, M., et al. (2017). Increased-order aeroservoelastic modeling in practice. In *Proceedings of the International Forum on Aeroelasticity and Structural Dynamics*. pp. 2017–165.

[18] Reyes, M., Climent, H., Karpel, M., et al. (2019). Examples on increased-order aeroservoelastic modeling. *CEAS Aeronautical Journal*, 10(4), 1071–1087. ISSN 1869-5590. doi:10.1007/s13272-019-00361-w.

[19] Wang, P., Wu, Z., and Yang, C. (2023). A modified frequency–time domain method for nonlinear aeroelastic systems with initial conditions. *Journal of Sound and Vibration*, 566, 117899. ISSN 0022-460X. doi:https://doi.org/10.1016/j.jsv.2023.117899.

[20] Conner, M., Tang, D., Dowell, E., et al. (1997). Nonlinear behavior of a typical airfoil section with control surface freeplay: A numerical and experimental study. *Journal of Fluids and Structures*, 11(1), 89–109. ISSN 0889-9746. doi:https://doi.org/10.1006/jfls.1996.0068.

[21] Liu, L. and Dowell, E. H. (2005). Harmonic balance approach for an airfoil with a freeplay control surface. *AIAA Journal*, 43(4), 802–815. doi:10.2514/1.10973.

[22] Abdelkefi, A., Vasconcellos, R., Nayfeh, A. H., et al. (2013). An analytical and experimental investigation into limit-cycle oscillations of an aeroelastic system. *Nonlinear Dynamics*, 71(1), 159–173. ISSN 1573-269X. doi:10.1007/s11071-012-0648-z.

COPYRIGHT STATEMENT